Atom-By-Atom Quantum State Control in Adatom Chains on a Semiconductor

Stefan Fölsch,[1] Jianshu Yang,[1] Christophe Nacci,[1] and Kiyoshi Kanisawa[2]

[1]*Paul-Drude-Institut für Festkörperelektronik, Hausvogteiplatz 5-7, 10117 Berlin, Germany*

[2]*NTT Basic Research Laboratories, NTT Corporation, 3-1 Morinosato Wakamiya, Atsugi, Kanagawa, 243-0198, Japan*

(Received 5 May 2009; published 27 August 2009)

The vertical manipulation of native adatoms on a III–V semiconductor surface was achieved in a scanning tunneling microscope at 5 K. Reversible repositioning of individual In atoms on InAs(111)A allows us to construct one-atom-wide In chains. Tunneling spectroscopy reveals that these chains host quantum states deriving from an adatom-induced electronic state and substantial substrate-mediated coupling. Our results show that the combined approach of atom manipulation and local spectroscopy is capable to explore atomic-scale quantum structures on semiconductor platform.

DOI: 10.1103/PhysRevLett.103.096104 PACS numbers: 68.37.Ef, 68.47.Fg, 73.20.At, 81.16.Ta

The ongoing miniaturization of semiconductor devices has reached a level where the exact number and spatial distribution of dopant atoms in the structure becomes a crucial factor for device performance [1]. Besides the improvement of existing device concepts by precisely controlling the doping process at the atomic scale [2], new directions are currently explored aiming at individual dopant atoms as functional units. Examples include the charge-state manipulation of isolated and coupled atoms [3], electron transport through the localized states of single dopants [4], and the coupling between dopant-based spins as a model system for quantum computation [5]. To disclose the effect of interatomic coupling in a semiconductor environment, an experimental approach combining the capabilities of local characterization and manipulation of matter at the atomic scale is desirable.

In this Letter, we show for the first time the reversible repositioning of native adatoms on a III–V semiconductor surface by vertical manipulation [6,7] in a scanning tunneling microscope (STM), i.e., by transferring individual atoms from the surface to the STM tip and vice versa. This allows us to assemble cation atom chains by adding one atom at a time and to follow the emergence of chain-localized electronic quantum states by scanning tunneling spectroscopy (STS). A linear-combination-of-atomic-orbitals (LCAO) model captures the effect of interference among the chain atoms and reproduces the observed molecular-orbital-like state densities. Our results document the extension of scanning-probe-based nanostructure assembly and spectroscopy to the material class of semiconductors. Besides tip-induced single-atom substitution achieved on Si [8] and GaAs surfaces [9], atom manipulation involving single atomic building blocks has not yet been achieved in semiconductor systems.

An ultrahigh vacuum (UHV) STM system operated at 5 K was used to carry out experiments on InAs(111)A grown by molecular beam epitaxy (MBE) [10]. The InAs(111)A surface is In-terminated and involves a (2×2) In-vacancy reconstruction. Earlier STM and density-functional theory (DFT) work revealed the stability of this reconstruction and showed that the MBE-grown surface exhibits native In adatoms residing on the vacancy sites [11]. STS measurements [13] further indicated that the In adatom acts as a donor supplying one electron to the conduction band, similar to the charge state found for native cation adatoms on epitaxial $In_{0.53}Ga_{0.47}As(111)A$ [14]. The STM topograph in Fig. 1(a) shows a surface area with two In adatoms imaged as protrusions with an apparent height of 0.6 Å. Figure 1(b) shows a single adatom at enhanced gray scale to indicate the surface reconstruction with In surface atoms imaged as protrusions

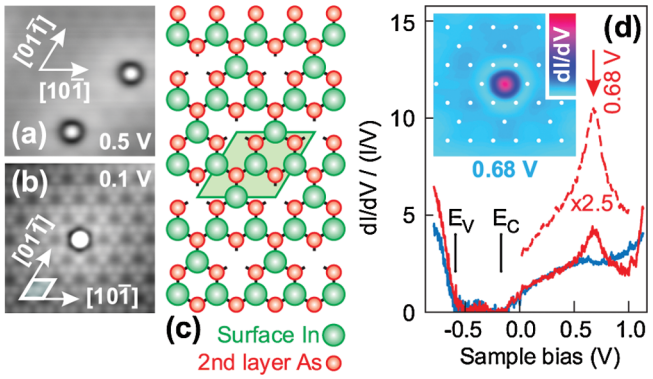

FIG. 1 (color). (a) Constant-current STM image (54 Å × 54 Å, 1 nA, 0.5 V) with two native In adatoms on InAs(111)A. (b) Enhanced gray scale image (54 Å × 54 Å, 2 nA, 0.1 V) indicating the adatom position relative to the (2×2) In-vacancy reconstruction. (c) Stick-and-ball model of the first two atomic layers; the rhombic surface unit cell is indicated in (b) and (c). (d) $dI/dV/(I/V)$ spectra yielding the LDOS measured with the tip over the surface (blue) and over the adatom (red). The red spectrum reveals an adatom-derived state at 0.68 eV above E_F; resonant dI/dV mapping [27 Å × 27 Å inset, set point 0.1 nA, 0.68 V, surface In atom positions marked by white dots] shows that the adatom state density is centered at the atomic position. All dI/dV measurements at constant tip height, lock-in modulation and frequency: 20 mV_{pp}, 670 Hz.

and vacancies as depressions [11]. A stick-and-ball model of the first two atomic layers is shown in Fig. 1(c). Figure 1(d) adds $dI/dV/(I/V)$ spectra detected with the STM tip positioned over the surface (blue) and over the adatom (red). We use the normalized differential tunneling conductance $dI/dV/(I/V)$ as a dimensionless measure of the surface local density of states (LDOS) [15]. The blue spectrum is in accord with previous studies [12] indicating a band gap of 0.42 eV and the conduction band minimum at about 0.2 eV below E_F. Fermi level pinning in the conduction band is a generic property of InAs surfaces and leads to charge accumulation at the surface [16]. The red spectrum in Fig. 1(d) detected over the adatom reveals a resonance at 0.68 V which we interpret as an unoccupied state deriving from atomic orbitals of the In adatom. Spatial dI/dV mapping at the resonance energy and at constant tip height [inset in panel (d)] verifies that the adatom LDOS distribution is isotropic and centered at the atom position.

We find that In adatoms can be reversibly repositioned by vertical manipulation to form compact structures (atoms occupying nearest-neighbor vacancy sites separated by $a_0\sqrt{2} = 8.57$ Å, a_0: cubic InAs lattice constant) or more open structures of various shape and size [17]. The STM images in Figs. 2(a) and 2(b) exemplify a single-atom pick-up event achieved by placing the tip over the marked atom, applying a sample bias of +1.25 V, moving the tip toward the surface, and retracting it back to the initial height (all tip displacements Δz quoted below relate to set point parameters of 0.1 nA and 0.5 V). Figure 2(c) details the tunnel current detected during approach (red) and retraction (blue): Apart from its exponential dependence on Δz, the tunnel current shows a sharp drop at −3.0 Å during approach (denoted as "P"), which is associated with the atom hopping from the surface to the tip apex. Similar current response curves are routinely obtained at positive sample biases down to a threshold of ~0.7 V. In contrast, surface-to-tip transfer is not attainable at negative bias suggesting that the tip-induced electric field is important for the process.

To analyze this further, the tunnel current was detected while placing the tip at reduced height and bias over an adatom, turning off the feedback loop and switching the bias to a constant positive value >0.7 V. Figure 2(g) shows exemplary current traces at three different junction settings corresponding to three different voltages at $\Delta z = -3$ Å, indicating that the elapsed time τ prior to transfer (evidenced by a current drop >1 order of magnitude) markedly decreases with increasing bias (and increasing current in the μA regime). Figure 2(h) shows the probability distribution of the elapsed time extracted from 134 independent pick-up events at junction settings with Δz between −2.73 Å and −3.05 Å and biases between 1.03 and 1.35 V. To include data obtained at different junction settings, the normalized quantity $\tau/\langle\tau\rangle$ is plotted ($\langle\tau\rangle$:

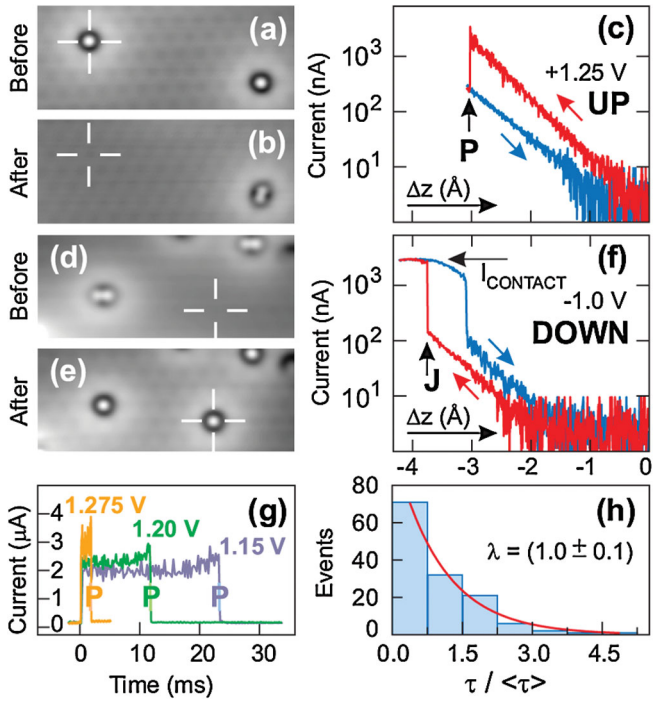

FIG. 2 (color). (a),(b) STM images (105 Å × 43 Å, 0.1 nA, 0.5 V) documenting single-atom surface-to-tip transfer (a) before and (b) after tip approach toward the marked adatom at 1.25 V sample bias. (c) Current versus tip displacement Δz during approach (red) and retraction (blue) indicating the pick-up event (P) at $\Delta z = -3.0$ Å (initial set point here and in the following: 0.1 nA, 0.5 V). (d),(e) STM images showing tip-to-surface back transfer (d) before and (e) after moving the tip at −1.0 V toward the marked vacancy site; corresponding current-vs-Δz curves (f) indicate a jump to contact (J) during approach. (g) Current traces measured with the tip over an adatom at fixed junction settings of $\Delta z = -3$ Å and positive biases as indicated showing different delay times τ prior to transfer. (h) Probability distribution of the normalized delay time $\tau/\langle\tau\rangle$ obtained at various settings with $\Delta z \in [-2.73\ \text{Å}, -3.05\ \text{Å}]$ and biases $\in [1.03\ \text{V}, 1.35\ \text{V}]$; the exponential decay indicates a statistical surface-to-tip transfer process.

mean elapsed time at a fixed setting). The exponential decay with a normalized decay constant equal to one indicates a statistical process, as found earlier in STM-induced activation by inelastic electron tunneling (IET) triggering, e.g., single-molecule dissociation [18] and vertical atom manipulation [7,19]. We thus associate the reversible manipulation observed here with a double-minimum potential scenario [19] where the surface-to-tip transfer is due to IET-induced vibrational excitation assisted by the tip-induced electric field acting on the positively charged In/InAs(111)A adatom. The observed bias threshold of ~0.7 V required for surface-to-tip transfer suggests that under zero-field conditions the In atom binding to the surface is clearly larger than to the tip apex.

The reversed transfer process at negative sample bias is illustrated in Figs. 2(d) [before tip approach to a vacancy

site] and 2(e) [after putting an In atom back down at the marked position]. The corresponding tunnel current curves in Fig. 2(f) indicate the formation of a tip-surface point contact during approach (evidenced by the jump in current labeled as "J" followed by a saturated current) while the contact eventually breaks during retraction, see sharp current drop and exponential decay in the vacuum tunneling regime. Single In atoms can be reproducibly deposited also at zero bias. This suggests that (i) the process is governed by short-range adhesive forces rather than by the tip-induced electric field, and (ii) at zero field adatom-surface binding is larger than adatom-tip binding (cf. discussion above). Earlier work showed that short-range adhesive forces lead to single-atom tip-to-surface transfer when an STM tip is brought into contact with a noble metal surface [20]; surface-to-tip back transfer, however, was not attainable in those metallic systems. Note also that lateral atom sliding [6] as commonly used on metal substrates does not permit to reposition In/InAs(111)A adatoms (the present system presumably involves ionic bonding character between the charged adatom and the polar (111) surface whose (2×2) reconstruction is driven by surface dangling bond saturation [21]).

The manipulation of single In adatoms allows us to explore the electronic properties of In chains atom by atom. The STM images in Fig. 3(a) demonstrate the assembly of a compact In_6 chain by starting with a monomer (left) and successively adding one atom at a time along the $[10\bar{1}]$ direction. The corresponding $dI/dV/(I/V)$ spectra in Fig. 3(b) were detected with the tip centered over the respective atoms indicated in (a). It is found that the atomic resonance at 0.68 V for the monomer gradually shifts towards E_F when N is increased. For the dimer, both atoms yield identical resonance peaks. For longer chains, the resonance magnitude is decreased when probing outer compared to inner atoms whereas the peak shape and position remain the same. Obviously, the downward shift in energy indicates an along-chain linking of the atomic state resulting in the formation of a chain-localized quantum state. It is tempting to interpret this behavior within a physical chemistry textbook framework as the formation of the bonding ground-state orbital in an artificial linear molecule, as applied earlier to describe confined states in metal-on-metal adatom chains [22,23].

To test the adequacy of this simple picture, spatial dI/dV maps of In chains were measured at constant tip height probing the lateral LDOS variation along the tip trajectory. Figure 3(c) shows the result obtained for a In_5 chain with the bias tuned to the ground-state resonance. As evident, the dI/dV signal is maximum at the center atom and successively decreased at the outer atoms. This behavior is consistent with the density of an LCAO ground-state wave function which for $N = 5$ has the LCAO coefficients $c_3 = 1/\sqrt{3}$ for the center atom, $c_2 = c_4 = 1/2$ for the center atom's next neighbors, and $c_1 = c_5 = 1/\sqrt{12}$ for

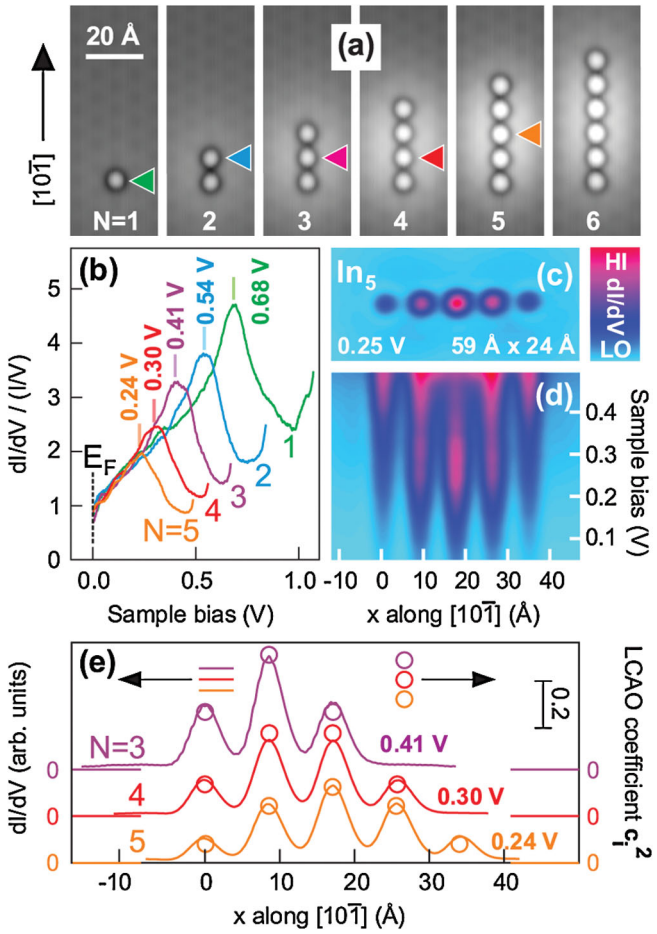

FIG. 3 (color). (a) STM images (33 Å × 84 Å, 0.1 nA, 0.1 V) showing the successive assembly of a In_6 chain by vertical atom manipulation. (b) $dI/dV/(I/V)$ spectra for In_N chains ($N = 1$ to $N = 5$) with the tip centered over the atoms indicated in (a). (c) Constant-height dI/dV map (set point 0.2 nA, 0.25 V) for In_5 with the bias tuned to the resonance energy. (d) Corresponding bias dependency of the along-chain dI/dV modulation indicating envelope functions with a single lobe between 0.2 and 0.3 V (ground state) and with two lobes between 0.4 and 0.5 V (first excited state). (e) Resonant along-chain dI/dV profiles for $N = 3$ to 5 measured at identical constant tip height; for clarity, the profiles are offset along y. The on-atom-centered dI/dV maxima agree well with the corresponding squared LCAO coefficients c_i^2 (indicated by circles and plotted along the right-hand side y axis).

the outermost atoms. Figure 3(d) adds the bias dependency of the along-chain dI/dV modulation and verifies that the characteristic ground-state signature in Fig. 3(c) is resonant between 0.2 and 0.3 V, whereas at higher bias the dI/dV signal decays at the center atom and accumulates at the outer atoms. We attribute this observation to the emergence of the first excited In_5 "molecular orbital" (MO) state having a nodal plane at the center atom position. In the range of higher bias (>0.5 V for In_5), we find that the excited MO type states are superimposed by a different

type of surface states most likely deriving from adatom-induced localization effects [14].

At this point, we focus on the well separated ground-state resonances and their characteristic along-chain dI/dV modulation indicated by the profiles in Fig. 3(e), measured for $N = 3$ to $N = 5$ at identical constant tip height. Within the LCAO model, the MO state density is proportional to the squared sum $\sum_{i=1}^{N} c_i \psi_i$ of N atomic orbitals ψ_i, each weighted by a corresponding coefficient c_i. The measured profiles show that the LDOS probed along the constant-height tip trajectory is predominantly localized at the atomic positions. Thus, within the LCAO picture the leading terms are those weighted by c_i^2 whereas the mixed terms weighted by $c_i c_j$ $(i \neq j)$ only yield a minor contribution to mimic the measured LDOS variation. Circles in Fig. 3(e) mark the corresponding values of the squared coefficients c_i^2 (see right-hand side y axis) and agree well with the on-atom-centered maxima of the dI/dV profiles. The LCAO model thus captures the main features of interference between the chain atoms and reproduces the squared envelope function of the bonding ground-state orbital.

In contrast to previous STS work on self-assembled Fe/InAs(110) [24] and Au/Si(553) chain structures [25] indicating a complex site-specific hybridization between adatom and substrate-derived states, the present observations are consistent with an along-chain linking of equivalent atomic building blocks. Regarding the substantial interatomic spacing of 8.57 Å present here it appears that substrate-mediated coupling is at work rather than direct coupling. We assume that the enhancement in substrate-mediated coupling as compared to metal-on-metal systems [26] originates from the generic bonding and electronic properties of the III–V semiconductor InAs, yielding a substantially larger screening length and a larger wavelength of quasifree electronic states at energies $\in [E_F, +0.7\ \mathrm{eV}]$ in the conduction band regime [12]. Future theoretical work is desirable to gain a deeper understanding of interatomic coupling in nanostructures supported on a semiconductor surface, whose assembly by atom manipulation has now become feasible.

Financial support by the Japanese Agency of Science & Technology (JST) and the German Research Foundation (DFG) is gratefully acknowledged.

[1] P. A. Packan, Science **285**, 2079 (1999).
[2] T. Shinada, S. Okamoto, T. Kobayashi, and I. Ohdomari, Nature (London) **437**, 1128 (2005).
[3] K. Teichmann *et al.*, Phys. Rev. Lett. **101**, 076103 (2008); I. Kuljanishvili *et al.*, Nature Phys. **4**, 227 (2008).
[4] H. Sellier *et al.*, Phys. Rev. Lett. **97**, 206805 (2006), and references therein.
[5] B. E. Kane, Nature (London) **393**, 133 (1998); M. Y. Simmons *et al.*, Int. J. Nanotechnology **5**, 352 (2008).
[6] J. A. Stroscio and D. M. Eigler, Science **254**, 1319 (1991).
[7] D. M. Eigler, C. P. Lutz, and W. E. Rudge, Nature (London) **352**, 600 (1991).
[8] Y. Sugimoto *et al.*, Science **322**, 413 (2008).
[9] D. Kitchen, A. Richardella, J.-M. Tang, M. E. Flatté, and A. Yazdani, Nature (London) **442**, 436 (2006).
[10] 20-nm-thick undoped InAs layers were grown on InAs(111)A under standard MBE conditions [11] and subsequently capped by arsenic. Loading the samples into the STM system and decapping them by annealing in UHV at 630 K yielded the same surface features as for MBE-grown and *in situ* investigated samples [11,12]. Chemically etched W tips were used and cleaned in UHV by electron beam heating.
[11] A. Taguchi and K. Kanisawa, Appl. Surf. Sci. **252**, 5263 (2006).
[12] K. Kanisawa, M. J. Butcher, H. Yamaguchi, and Y. Hirayama, Phys. Rev. Lett. **86**, 3384 (2001).
[13] K. Kanisawa and T. Fujisawa, Hyomen Kagaku **29**, 747 (2008) (in Japanese).
[14] S. Perraud, K. Kanisawa, Z.-Z. Wang, and T. Fujisawa, Phys. Rev. Lett. **100**, 056806 (2008).
[15] R. M. Feenstra, Surf. Sci. **299–300**, 965 (1994).
[16] L. Ö. Olsson, C. B. M. Andersson, M. C. Håkansson, J. Kanski, L. Ilver, and U. O. Karlsson, Phys. Rev. Lett. **76**, 3626 (1996).
[17] The vacancy sites are the only stable surface lattice sites of In adatoms after tip-to-surface transfer. A success rate of 81% (71%) was found in 376 (418) attempts of surface-to-tip (tip-to-surface) transfer at positive (negative) sample bias as described below.
[18] B. C. Stipe *et al.*, Phys. Rev. Lett. **78**, 4410 (1997).
[19] R. E. Walkup, D. M. Newns, and Ph. Avouris, Phys. Rev. B **48**, 1858 (1993); S. Gao, M. Persson, and B. I. Lundqvist, Phys. Rev. B **55**, 4825 (1997).
[20] L. Limot, J. Kröger, R. Berndt, A. Garcia-Lekue, and W. A. Hofer, Phys. Rev. Lett. **94**, 126102 (2005).
[21] K. W. Haberern and M. D. Pashley, Phys. Rev. B **41**, 3226 (1990).
[22] N. Nilius, T. M. Wallis, and W. Ho, Science **297**, 1853 (2002).
[23] S. Fölsch, P. Hyldgaard, R. Koch, and K. H. Ploog, Phys. Rev. Lett. **92**, 056803 (2004); J. Lagoute, X. Liu, and S. Fölsch, Phys. Rev. B **74**, 125410 (2006).
[24] T. Matsui, Chr. Meyer, L. Sacharow, J. Wiebe, and R. Wiesendanger, Phys. Rev. B **75**, 165405 (2007).
[25] J. N. Crain and D. T. Pierce, Science **307**, 703 (2005).
[26] N. Nilius, T. M. Wallis, M. Persson, and W. Ho, Phys. Rev. Lett. **90**, 196103 (2003); A. Sperl, J. Kröger, R. Berndt, A. Franke, and E. Pehlke, New J. Phys. **11**, 063020 (2009).